



저작자표시-비영리-변경금지 2.0 대한민국

이용자는 아래의 조건을 따르는 경우에 한하여 자유롭게

- 이 저작물을 복제, 배포, 전송, 전시, 공연 및 방송할 수 있습니다.

다음과 같은 조건을 따라야 합니다:



저작자표시. 귀하는 원저작자를 표시하여야 합니다.



비영리. 귀하는 이 저작물을 영리 목적으로 이용할 수 없습니다.



변경금지. 귀하는 이 저작물을 개작, 변형 또는 가공할 수 없습니다.

- 귀하는, 이 저작물의 재이용이나 배포의 경우, 이 저작물에 적용된 이용허락조건을 명확하게 나타내어야 합니다.
- 저작권자로부터 별도의 허가를 받으면 이러한 조건들은 적용되지 않습니다.

저작권법에 따른 이용자의 권리는 위의 내용에 의하여 영향을 받지 않습니다.

이것은 [이용허락규약\(Legal Code\)](#)을 이해하기 쉽게 요약한 것입니다.

[Disclaimer](#)

의학박사 학위논문

혈관형성억제제로 치료받은 재발성 교모종  
환자에서 혈관크기 및 관류영상을 이용한  
vascular habitat 을 통한 예후 예측: 전향적  
연구에서의 검증

Vessel size and perfusion-derived vascular habitat  
refines prediction to antiangiogenic agent in  
recurrent gliomas: validation in a prospective  
population

울산대학교 대학원  
의학과  
김민재

혈관형성억제제로 치료받은 재발성 교모종  
환자에서 혈관크기 및 관류영상을 이용한  
vascular habitat 을 통한 예후 예측: 전향적  
연구에서의 검증

지도교수 박지은

이 논문을 의학박사학위 논문으로 제출함

2022 년 2 월

울산대학교 대학원  
의학과  
김민재

김민재의 의학박사학위 논문을 인준함

심사위원 김 호 성 인

심사위원 박 지 은 인

심사위원 이 상 민 인

심사위원 정 승 채 인

심사위원 최 병 세 인

울산대학교 대학원

2022 년 2 월

## 국문요약

연구제목: 혈관형성억제제로 치료받은 재발성 교모종 환자에서 혈관크기 및 관류영상을 이용한 vascular habitat을 통한 예후 예측: 전향적 연구에서의 검증

연구배경: 혈관형성억제제는 모든 재발성 교모종 환자에서 효과를 보이지 않지만 혈관형성억제제에 대한 치료 반응 평가를 위한 영상의학적인 지표는 현재 제한적이다. 이에 혈관형성억제제로 치료 받은 재발성 교모종 환자에서 종양진행시간 예측을 위해 관류 및 혈관 크기 정보를 이용한 vascular habitat을 개발 및 검증하고자 하였다.

연구방법: 본 연구는 혈관형성억제제로 치료 시작 전 dynamic susceptibility contrast 및 vessel architectural imaging을 시행한 재발성 교모종 환자 69명을 대상으로 하였다. Vascular habitat은 vessel size index (VSI) 와 relative cerebral blood volume (rCBV) 정보를 이용하였다. Vascular habitat과 종양진행시간과의 연관성을 Cox 비례 위험 회귀 분석을 통해 분석하였다. 또한, 전향적으로 모집된 환자군 (ClinicalTrials.gov identifier; NCT04143425) 에서 vascular habitat을 이용하여 치료반응군을 분류하고자 하였다.

연구결과: rCBV 및 VSI를 이용하여 high angiogenic, intermediate angiogenic 및 low angiogenic habitat을 구성하였다. High angiogenic 및 intermediate angiogenic habitat은 유의하게 짧은 종양진행시간을 예측하였다 (위험 비율: 2.78 및 1.82, largest  $P = .003$ ). High angiogenic habitat은 rCBV보다 높은 예측력을 보였다 (위험 비율: 2.15). High angiogenic 및 intermediate angiogenic habitat을 합친 vascular habitat은 rCBV보다 약간 높은 concordance probability index를 보였다. Vascular habitat은 전향적 환자군에서 치료반응군과 비반응군으로 분류하였다 ( $P = .059$ ).

결론: 관류 및 혈관크기 정보를 이용한 vascular habitat은 혈관형성억제제로 치료받은 재발성 교모세포종 환자에서 종양진행시간을 예측하였고 전향적 환자군에서 치료 반응군을 분류하였다.

## 목차

국문요약 .....	i
표 및 그림 차례 .....	iii
서론 .....	1
연구대상 및 연구방법 .....	2
1. Study population .....	2
2. MRI protocol and image processing .....	3
3. Definition of rCBV and vessel size .....	4
4. Vascular habitats .....	5
5. Response assessment and time to progression .....	6
6 Statistical analysis .....	7
결과 .....	8
1. Patient demographics .....	8
2. Vascular habitats associated with TTP in the derivation set .....	10
3. Vascular habitats and progression type .....	13
4. Stratification using vascular habitats .....	14
5. Validation in a prospective clinical cohort .....	16
고찰 .....	17
결론 .....	19
참고문헌 .....	20
영문요약 .....	24

## 표 및 그림 차례

Table 1. Clinical characteristics of the patients .....	9
Table 2. Imaging parameters and vascular habitats to predict TTP in recurrent glioblastoma treated with bevacizumab .....	11
Figure 1. Flow diagram of the patient selection protocol .....	3
Figure 2. The overall process of vascular habitat analysis.....	6
Figure 3. Representative case of vascular habitat predicting TTP.....	12
Figure 4. Risk stratification based on high and intermediate angiogenic habitat in the derivation set.....	15
Figure 5. Risk stratification based on vascular habitats in the validation set .....	17

## 서론

Anti-angiogenic therapy represents a mainstay in the treatment of recurrent glioblastomas, and vascular normalization of bevacizumab is thought to enhance the effect of simultaneously administered chemotherapy, radiation therapy and immunotherapy <sup>1,2</sup>. However, anti-angiogenic therapy may not benefit all patient subsets <sup>3-6</sup> and it is important to identify imaging biomarker that accurately predicts treatment effect of anti-angiogenic therapy in order to aid patient selection.

Previous studies reported that pretreatment cerebral blood volume (CBV) derived from dynamic susceptibility contrast (DSC) MRI predicted progression free survival and overall survival potentially enabling patient stratification <sup>7-9</sup>. Recently, vessel size on vessel architecture imaging (VAI) estimated by comparing different sensitivity of gradient-echo (GRE) and spin-echo (SE) to the susceptibility effect of microscopic and macroscopic vessels allowed identification of responders to anti-angiogenic therapy <sup>10</sup>. On a longitudinal analysis, improved oxygenation and reduced vessel size were observed in patients with recurrent glioblastomas treated with bevacizumab <sup>10</sup>. Nonetheless, studies were limited in their depiction of spatial arrangement of vascular information.

Spatial information of tumor microvasculature, especially in recurrent glioblastoma, with tumor heterogeneity mixed with treatment effect and complex interplay of vascular mimicry, co-option, and vasculogenesis <sup>11</sup>, may enable more precise prediction of tumor progression and treatment response to anti-angiogenic therapy <sup>12</sup>. Distinct tumor habitats through parcellation <sup>13</sup> can be applied to analyze multiple imaging parameters, which may identify and quantify tumor subregions of treatment resistance. We hypothesized that parcellation of DSC-derived relative CBV (rCBV) and VAI-derived parameter could potentially identify vascular habitats that can predict treatment response to anti-angiogenic therapy in patients with recurrent glioblastomas. Therefore, the aim of this study was to develop and validate vascular



habitats based on rCBV and vessel size to predict time to progression (TTP) in patients with recurrent glioblastomas treated with bevacizumab.

## 연구대상 및 연구방법

### 1. Study population

This study was approved by the institutional review board of Asan Medical Center, and the requirement to obtain informed consent was waived for patients included in the derivation set. A prospective observational cohort (ClinicalTrials.gov identifier; NCT04143425) was recruited for validation set, and written informed consent was obtained from all patients. **Figure 1** shows the patient inclusion process. For derivation set, the neuro-oncology database of Asan Medical Center was retrospectively reviewed between May 2018 and October 2020. Inclusion criteria were as follows: (a) patients with histopathological diagnosis of glioblastomas, either isocitrate dehydrogenase (IDH) mutant or wild type; (b) subsequently diagnosed as recurrence by the clinic-radiologic consensus after standard treatment of surgical resection, concurrent chemoradiotherapy (CCRT) and adjuvant temozolomide; (c) treated with bevacizumab (Avastin; Roche, Welwyn Garden City, England; 10 mg per kilogram body weight) alone or in combination with other agents (temozolomide, irinotecan, oxaliplatin, or 5-fluorouracil with variable regimen); (d) underwent MRI with DSC, VAI and diffusion-weighted imaging prior to initiation of bevacizumab; and (e) underwent at least one follow up MRI to determine treatment response. Of 124 eligible patients, 45 patients who did not have adequate pretreatment or sequential follow-up MRI, 6 patients who received other secondary treatment including re-operation, re-irradiation, or other immunotherapies, and 4 patients whose pretreatment MRI was longer than three months prior to the initiation of bevacizumab were excluded.

An independent validation set of prospectively enrolled, IDH-wild type glioblastomas treated with bevacizumab was used to evaluate the true clinical

performance and included patients followed up between February 2020 and August 2021. No patients were excluded and the final validation set consisted of 15 patients.

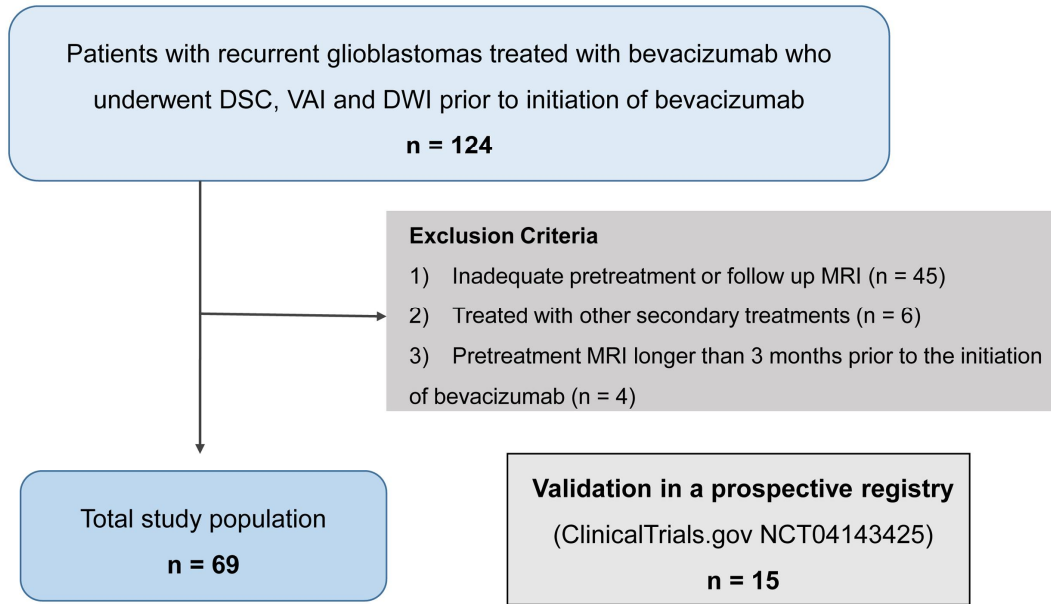


**Figure 1.** Flow diagram showing the patient selection protocol and the inclusion and exclusion criteria. DSC = dynamic susceptibility-weighted contrast imaging, VAI = vessel architectural imaging, DWI = diffusion-weighted imaging.

## 2. MRI protocol and image processing

The brain tumor imaging protocol obtained prior to the initiation of bevacizumab and at follow up included T2-weighted imaging, FLAIR imaging, T1-weighted imaging, diffusion-weighted imaging, simultaneous GRE-SE DSC perfusion, contrast-enhanced-T1-weighted imaging, and conventional DSC perfusion MRI. Simultaneous GRE-SE DSC-MRI was acquired using axial gradient-echo, spin-echo echo-planar images with repetition time 1.33 s, echo times 34 ms and 103 ms (respectively), slice thickness 5 mm, interslice distance 2.5 mm, in-plane resolution 1.70×1.70 mm, matrix size

128×128, 10 slices and 120 volumes. For simultaneous GRE–SE DSC perfusion, a dynamic bolus was administered as a standard dose of 0.1 mmol/kg gadoterate meglumine (Dotarem; Guerbet) delivered at a rate of 4 mL/s by a MRI-compatible power injector (Spectris; Medrad). The bolus of contrast material was followed by a 20 mL bolus of saline, injected at the same rate. For conventional DSC perfusion, a second, standard dose of 0.1 mmol/kg gadoterate meglumine was administered. The dynamic acquisition was performed with a temporal resolution of 1.5 s, and 60 dynamics were acquired.

### 3. Definition of rCBV and vessel size

The whole-brain rCBV, normalized to contralateral normal-appearing white matter, was calculated using numerical integration of the time concentration curve after correcting for contrast agent leakage. Leakage correction was performed using the method of Weisskoff et al. with further adaptations from Boxerman et al. 14, with leakage being estimated from the deviation in each voxel according to a non-leakage reference tissue response curve.

The vessel size index was chosen as a VAI parameter. Relative vessel size index was defined by  $\text{relative vessel size index} = \sqrt{\text{rCBV} \times \text{ADC}} \times \beta$ , where  $\beta$  is the slope of the long axis of the hysteresis curve, ADC is the apparent diffusion coefficient, and rCBV is relative cerebral blood volume obtained from the GRE signal normalized to contralateral normal-appearing white matter 10,15. Preprocessing for rCBV and vessel size was performed using the commercial software package (nordicICE v. 4.0.6; NordicNeuroLab, Bergen, Norway).

For the three-dimensional contrast-enhanced T1WI (3D CE-T1WI) and FLAIR data, skull stripping was done using an optimized algorithm (<https://github.com/MIC-DKFZ/HD-BET>) for heterogeneous MRI data with diverse pathology or post-treatment changes. Deep learning-based lesion segmentation was performed on the 3D CE-T1WI (enhancing tumor) and

FLAIR data (non-enhancing tumor) using a 3D UNet-based method (<https://github.com/MIC-DKFZ/nnUNet>) 16 from the PyTorch package version 1.1 in Python 3.7 ([www.python.org](http://www.python.org)). The region of interest included solid tumor consisting of FLAIR hyperintensity and contrast enhancing lesion, and necrotic portion was excluded. The 3D CE-T1WI and FLAIR images were co-registered to the rCBV and vessel size index maps using rigid transformations with six degrees of freedom in SPM package (version 12, [www.fil.ion.ucl.ac.uk/spm/](http://www.fil.ion.ucl.ac.uk/spm/)).

#### 4. Vascular habitats

All voxels from all segmented masks were first aggregated, and all voxels in the normalized CBV and vessel size index maps were split into clusters which were functionally coherent subregions within solid tumor. The individual voxels in each cluster were grouped based on their similarities and differences using K-means clustering algorithm with squared Euclidean distances between voxel intensities as the similarity metric. Finally, all the voxels from all the segmented masks in the normalized CBV maps and vessel size index were split into three clusters that were functionally coherent subregions. The cluster number was set as three as the lowest number to enable functionally coherent vascular subregions was preferred to avoid construction of an overparameterized model <sup>17</sup>.

Hence, three clusters were set: class 1 represented “high angiogenic habitat” with high CBV and vessel size index value; class 2 represented “intermediate angiogenic habitat” with intermediate CBV and vessel size index value; and class 3 represented “low angiogenic habitat” with low CBV and vessel size index value. All voxels were allocated into one of the three classes and were displayed as vascular habitats in the original image space. The range for boundary of vascular habitats was 3.14 – 6.83 for rCBV and 223.34 – 494.49 for vessel size index. The overall process of vascular habitat analysis is shown in **Figure 2**.

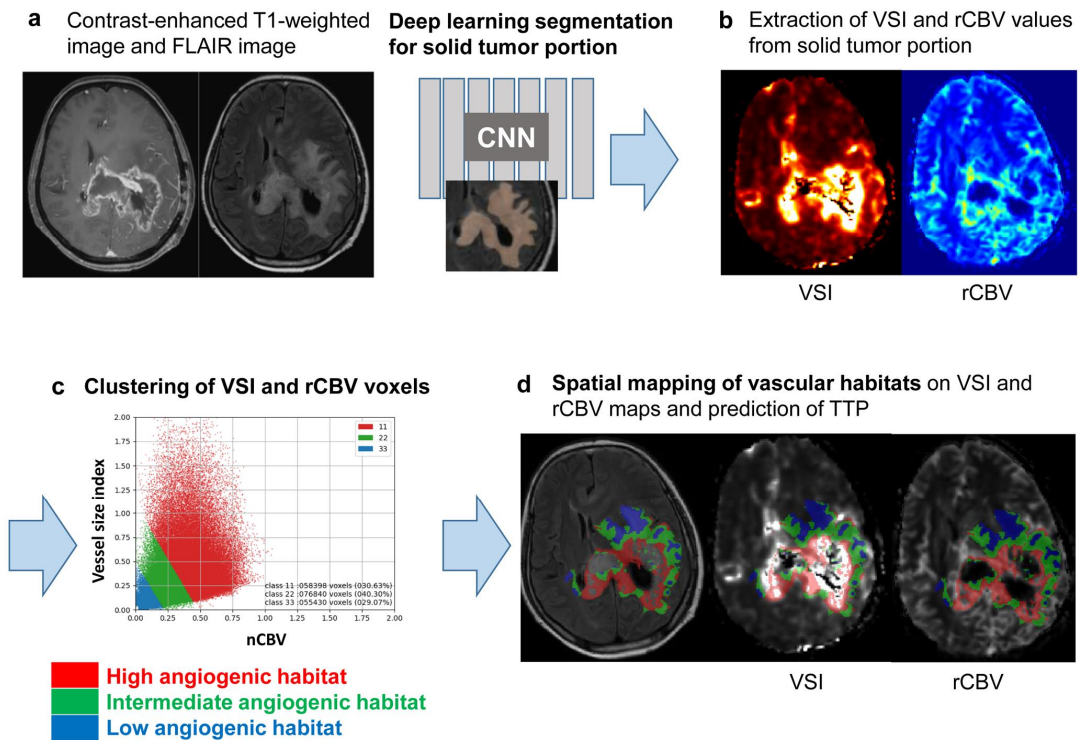


**Figure 2.** The overall process of vascular habitat analysis. A, Image acquisition, registration, and segmentation of FLAIR hyperintensity. B, Extraction of VSI and rCBV values from solid tumor portion. C, The cluster number was set to 3 to depict 3 different vascular habitats according to the combinations of VSI and rCBV parameters: high angiogenic, intermediate, and low angiogenic habitat. D, Voxels are shown as spatial habitats in the original image space. Associations of pretreatment vascular habitats with TTP were analyzed. FLAIR = fluid-attenuated inversion recovery image, CNN = convolutional neural network, VSI = vessel size index, rCBV = relative cerebral blood volume, TTP = time to progression.

## 5. Response assessment and time to progression (TTP)

Tumor progression was determined by the clinicoradiologic consensus between a neuro-oncologist (J.H.K. with 27 years of experience in neuro-oncology practice) and a neuro-radiologist (H.S.K. with 21 years of experience in neuro-oncology imaging) according to the Response

Assessment in Neuro-Oncology criteria<sup>18</sup>. TTP from the initiation of bevacizumab to disease progression was analyzed.

Separately, the pattern of progression was classified by two neuroradiologists in consensus (J.E.P. and H.S.K. with 6 and 21 years of experience in neuro-oncologic imaging, respectively) at the time of progression accordingly to previous studies<sup>4,5,19</sup>. In brief, there were three patterns of progression: (a) local enhancing progression (focus of contrast enhancement at or within 3cm of the primary site), (b) diffuse nonenhancing progression (local contrast-enhancing tumor remains stable but an area of abnormal FLAIR hyperintensity beyond 3cm from the primary site appears) and (c) distant progression (new focus of contrast enhancement or area of abnormal FLAIR hyperintensity appears beyond 3cm from the primary site with intervening normal-appearing white matter).

## 6. Statistical Analysis

All results are reported as mean with standard deviation or range or median with interquartile ranges for continuous variables, and as frequencies or percentages for categorical variables. Differences in clinicopathological factors between the derivation and validation cohorts were assessed using the chi-square test for discrete variables and Student's *t*-test for continuous variables.

***Association of vascular habitats with TTP:*** Univariate analysis was performed to analyze the associations of imaging parameters or vascular habitats with TTP using Cox proportional hazard regression analysis. Hazard ratios indicate relative change in hazard that 1 unit increase in each parameter incurs, and 30000 voxels (30k voxels) were considered as 1 unit.

Concordance probability index (C-index) of the vascular habitat combining high and intermediate angiogenic habitats was calculated and compared with that of rCBV alone.

***Vascular habitats and progression type:*** Voxel numbers of the significant habitats identified in the univariate Cox regression were compared between

local enhancing pattern of progression and non-local patterns of progression (diffuse nonenhancing and distant progression) using Student's *t*-test.

***Stratification of patients using vascular habitat:*** For the significant habitat identified in the univariate Cox regression, an optimal cutoff for stratifying high- and low-risk groups was estimated using maxstat in R with 10-fold cross validation, which ensured unbiased prediction within the sample <sup>20</sup>.

Using this cutoff from the exploratory analysis, a habitat risk score was developed for risk stratification of patients in the validation set; each predictor was assigned a discrete score of 1 if it was higher than its cutoff, and 0 if it was lower. In both derivation and validation sets, patient stratification was demonstrated by calculating survival curves using Kaplan-Meier method and low- and high-risk groups or good or poor responder groups were compared using log-rank test.

All statistical tests were two-sided, and a *P* value < 0.05 was considered to indicate statistical significance. Statistical analyses were performed using R software version 3.4.3 (<https://www.r-project.org>).

## 결과

### 1. Patient demographics

The clinical characteristics of the patients in the derivation and validation sets are presented in Table 1. There were 69 patients included in the derivation set (mean age, 55.0 ± 12.5 years [range, 25–78]; 32 [46.4 %] women) and 15 patients in the validation set (mean age, 48.9 ± 10.5 years [range, 22–64]; 6 [40.0 %] women). No differences in sex, age, IDH mutation and O6-methylguanine-DNA methyltransferase (MGMT) promotor methylation status were noted between the derivation and validation sets. All patients in the validation set received bevacizumab in combination with other agents while 45 patients (65.2%) received bevacizumab monotherapy in the derivation set (*P* < .001).

Median follow-up period after bevacizumab treatment was 139.0 days (interquartile range [IQR], 90.0–262.3 days) for the derivation set and 129.0 days (IQR, 65.8–187.0 days) for the validation set ( $P = .19$ ). More patients showed progression following bevacizumab therapy in the derivation set (84.1 % (58/69) vs 60.0 % (9/15);  $P = .04$ ). The median time to progression was 159.9 days (IQR, 82.0–199.0) in the derivation set and 121.6 days (IQR, 34.0–192.0) in the validation set ( $P = .33$ ).

**Table 1. Clinical characteristics of the patients**

	Derivation set (n = 69)	Validation set (n = 15)	<i>P</i>
Age (years)	55.0 ± 12.5	48.9 ± 10.5	.08
No. of female patients	32 (46.4%)	6 (40.0%)	.65
IDH-wild type	52 (75.4%)	13 (86.7%)	.35
MGMT promoter status (methylated /unmethylated/NA)	23/24/22	5/9/1	.42
Mean time interval between the operation and imaging (days)	267.5 ± 511.8	182.4 ± 120.2	.33
Bevacizumab regimen (n)			< .001
Bevacizumab alone	45 (65.2%)	0 (0%)	
Bevacizumab plus chemotherapy	24 (34.8%)	15 (100%)	
Response			
Median follow-up period after bevacizumab treatment (days)	139.0 (90.0–262.3)	129.0 (65.8–187.0)	.12
Patients with progression (n)	58 (84.1%)	9 (60.0%)	.04
Median time to progression (days)	159.9 (82.0–199.0)	121.6 (34.0–192.0)	.33
Progression pattern			
Local enhancing (n)	22 (37.9%)	1 (11.1%)	
Diffuse nonenhancing (n)	25 (36.2%)	6 (66.7%)	
Distant progression (n)	11 (15.9%)	2 (22.2%)	



Note: Unless otherwise specified, data are expressed as the mean  $\pm$  standard deviation and numbers in parenthesis are the interquartile range. Abbreviations: IDH = isocitrate dehydrogenase, MGMT= O6-methylguanine-DNA methyltransferase, NA = not available.

## 2. Vascular habitats associated with TTP in the derivation set

The results of the univariate analysis of vascular habitats and imaging parameters in association with TTP are presented in **Table 2**. Amongst all predictors, high angiogenic habitat was most significantly associated with a shorter TTP (hazard ratio [HR], 2.78; 95% CI, 1.53 – 5.02;  $P < .001$ ). Intermediate angiogenic habitat was also significantly associated with a shorter TTP (HR, 1.82; 95% CI, 1.22 – 2.70;  $P = .003$ ). When evaluated in percentages, high angiogenic habitat (HR, 1.05; 95% CI, 1.01 – 1.09;  $P = .008$ ) and low angiogenic habitat (HR, 0.99; 95% CI, 0.97 – 1.00;  $P = .03$ ) were significantly associated with a shorter TTP but the associations were weaker. The representative cases are shown in **Figure 3**.

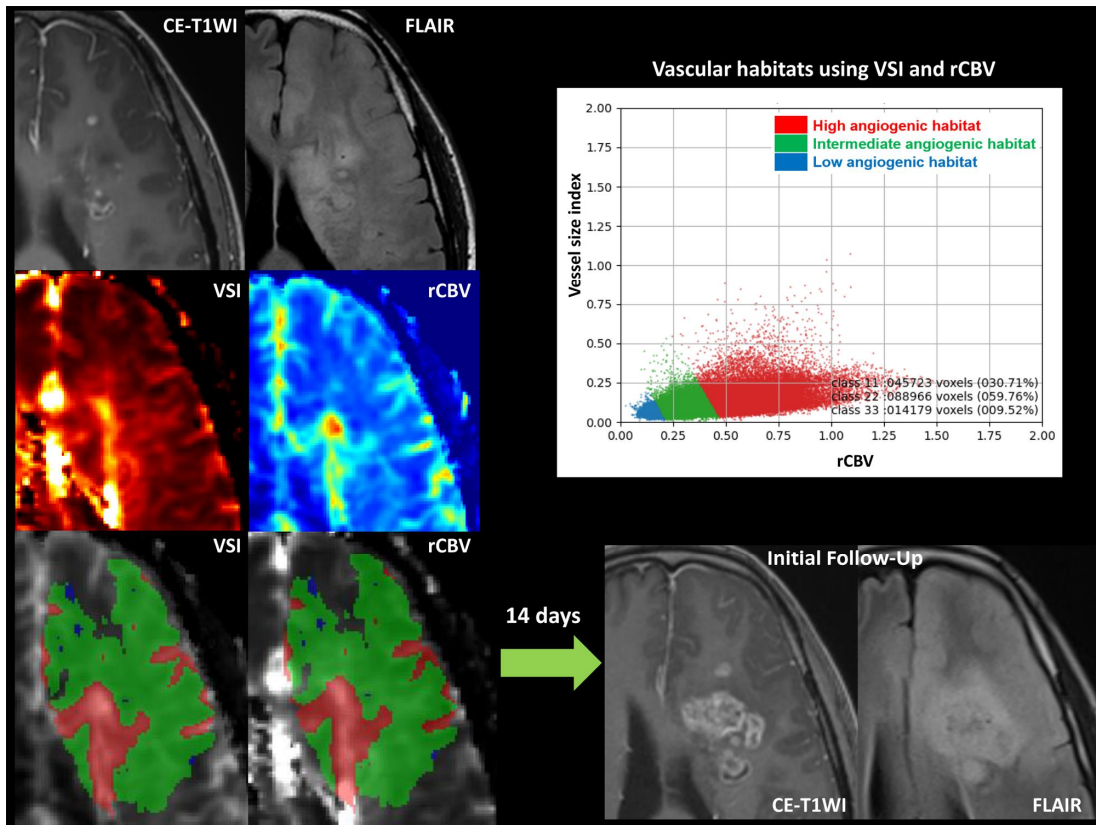
In single parameter analysis, pretreatment rCBV (HR, 2.15; 95% CI, 1.10 – 4.17;  $P = .02$ ) was significantly associated with a shorter TTP but the association was weaker than high angiogenic habitat evaluated in voxel numbers. The vessel size index (HR, 1.02; 95% CI, 1.00 – 1.04;  $P = .02$ ) was also significantly associated with a shorter TTP.

Table 2. Imaging parameters and vascular habitats to predict TTP in recurrent glioblastoma treated with bevacizumab

Imaging parameters	Hazard ratio	<i>P</i> value	<i>Z</i> statistic
Pretreatment rCBV	2.15 (1.10 – 4.17)	.02	2.26
Pretreatment VSI	1.02 (1.00 – 1.04)	.02	2.26
Pretreatment ADC	0.98 (0.96 – 1.01)	.20	-1.27
Vascular habitats (30k voxel numbers)			
High angiogenic	2.78 (1.53 – 5.02)	< .001	3.38
Intermediate angiogenic	1.82 (1.22 – 2.70)	.003	2.95
Low angiogenic	1.09 (0.95 – 1.25)	.21	1.26
Vascular habitats (%)			
High angiogenic	1.05 (1.01 – 1.09)	.008	2.66
Intermediate angiogenic	1.01 (1.00 – 1.03)	.10	1.65
Low angiogenic	0.99 (0.97 – 1.00)	.03	-2.12

Note: Hazard ratio for vascular habitats indicates the relative change in hazard ratio that a 1-unit (30, 000 voxels) or 1% increase in each vascular habit incurs.

Abbreviations: VAI = Vessel architectural imaging, rCBV = relative cerebral blood volume, VSI = Vessel size index, ADC = apparent diffusion coefficient.



**Figure 3A.** A 49 year old man with recurrent glioblastoma (IDH-wild type) showed high number of voxels of high and intermediate angiogenic habitats on the MRI prior to the initiation of bevacizumab therapy and time to progression following bevacizumab therapy was 14 days. IDH = isocitrate dehydrogenase.

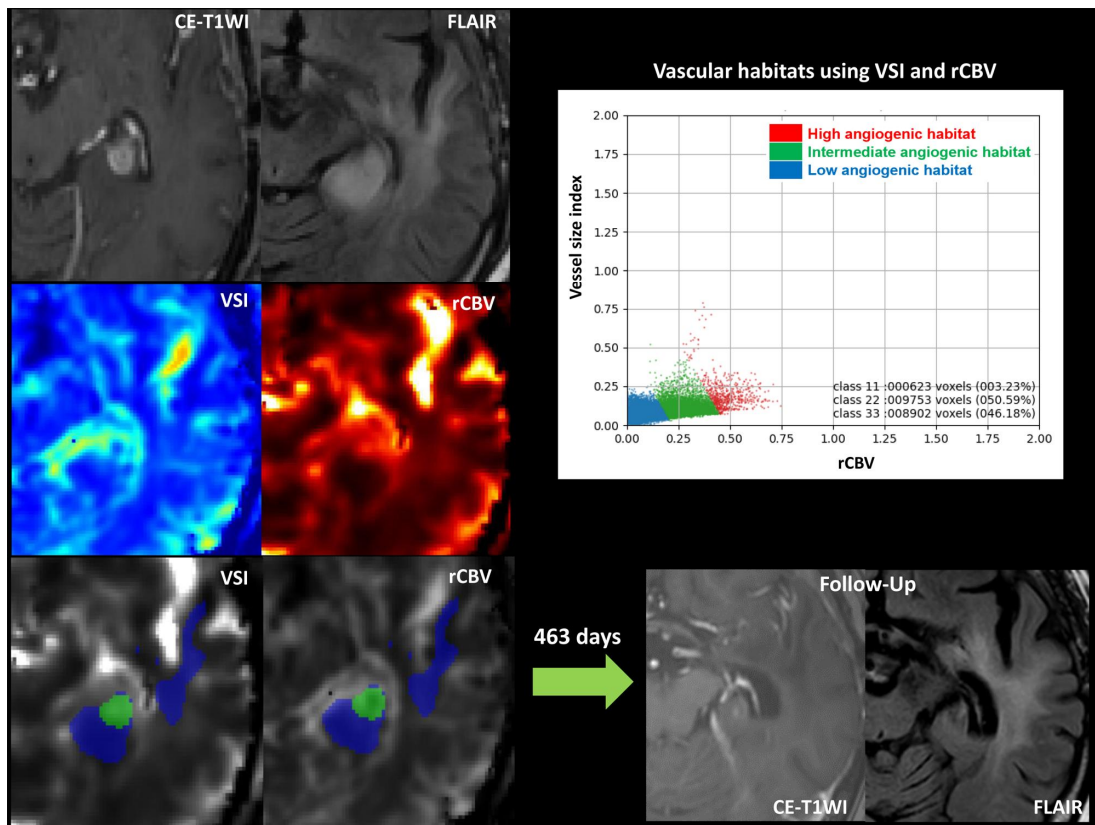


**Figure 3B.** A 64 year old woman with recurrent glioblastoma (IDH-wild type) showed small number of voxels of high and intermediate angiogenic habitats on the MRI prior to the initiation of bevacizumab therapy and time to progression following bevacizumab therapy was 463 days. IDH = isocitrate dehydrogenase.

### 3. Vascular habitats and progression type

Amongst 58 patients with progression following antiangiogenic therapy, there was 22 patients (22/58, 37.9%) with local enhancing pattern, 25 patients (25/58, 36.2%) with diffuse nonenhancing pattern and 11 patients (11/58, 15.9%) with distant pattern of progression. For local enhancing pattern of progression, there was a trend towards higher voxel numbers of high angiogenic habitat (mean  $\pm$  standard deviation;  $0.40 \pm 0.57$  vs  $0.24 \pm 0.39$ ,  $P = .22$ ) and intermediate angiogenic habitat ( $1.25 \pm 0.77$  vs  $1.18 \pm 0.66$ ,  $P = .71$ ) compared with non-local patterns of progression.

#### 4. Stratification using vascular habitats

The optimal vascular habitat cutoff for stratifying patients for treatment failure to bevacizumab was 1,262 voxels for high angiogenic habitat and 18,256 voxels for intermediate angiogenic habitat. There were 54 patients (78.3%, 54/69) stratified to be high risk based on high angiogenic habitat and 50 patients (72.5%, 50/69) stratified to be high risk based on intermediate angiogenic habitat. Risk stratification based on vascular habitats classified patients into high risk or low risk of tumor progression with a significant difference in the log-rank test for both high angiogenic habitat ( $P = .01$ ) and intermediate angiogenic habitat ( $P = .009$ ). The Kaplan–Meier survival curve and risk table based on vascular habitat risk stratification is shown in Figure 4. Patients were stratified to be poor responders if they were stratified to be high risk in high angiogenic and/or intermediate angiogenic habitats (risk score of 1 or 2), and there were 57 patients stratified to be poor responders using vascular habitats in the derivation set.

The C-index of vascular habitat combining high and intermediate angiogenic habitat (0.74; 95% CI, 0.62 – 0.83) was slightly higher than that of rCBV (0.72; 95% CI, 0.60 – 0.82).

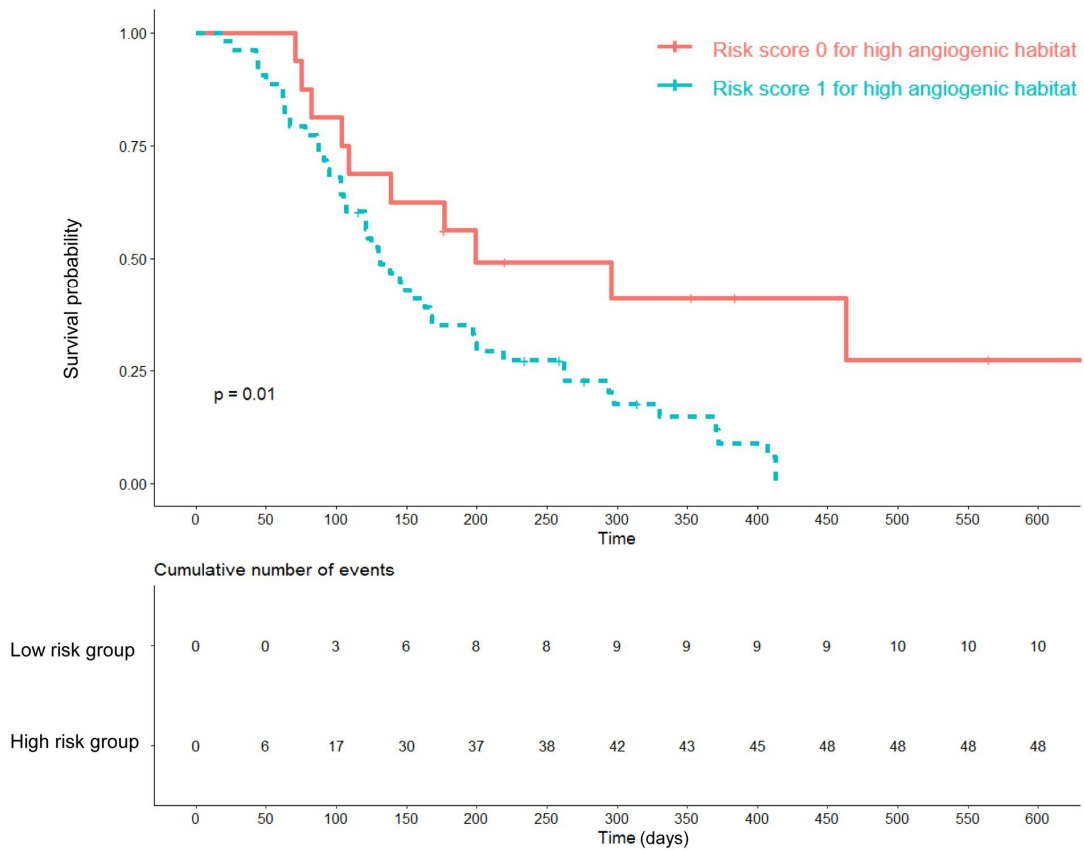


**Figure 4A.** Risk stratification based on high angiogenic habitat predicted treatment resistance to bevacizumab therapy in the derivation set.

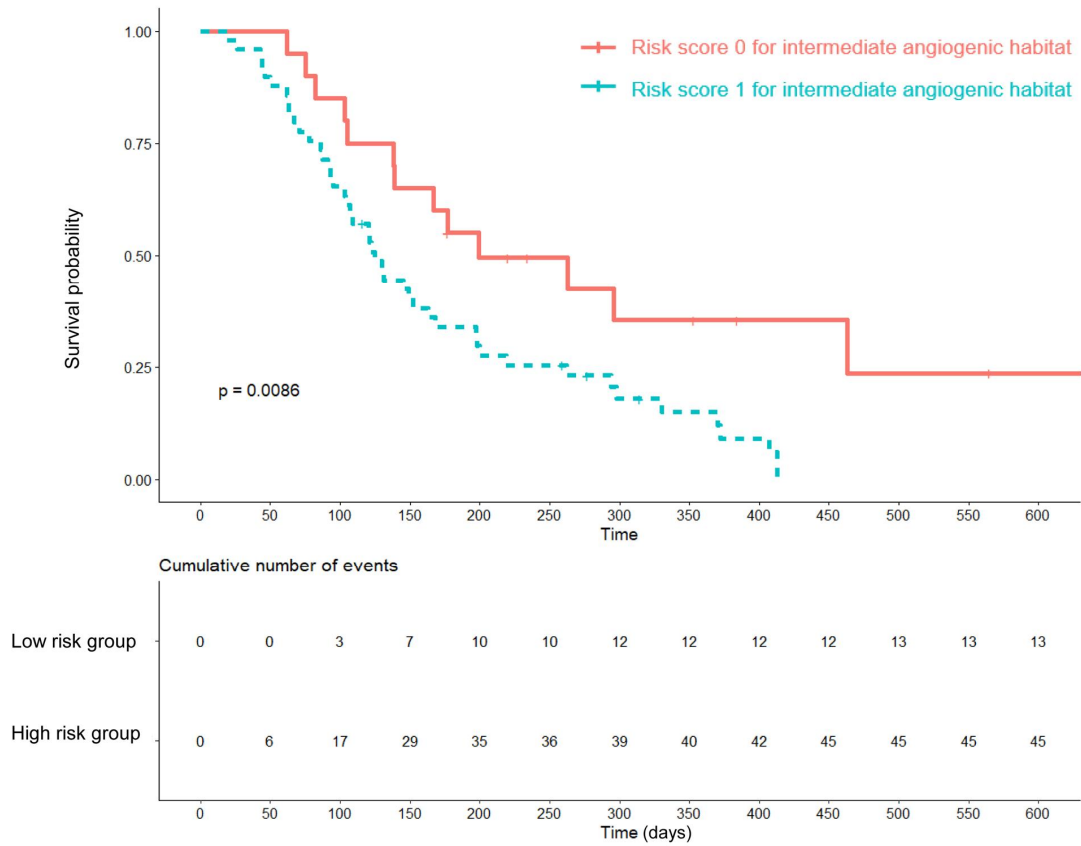


**Figure 4B.** Risk stratification based on intermediate angiogenic habitat predicted treatment resistance to bevacizumab therapy in the derivation set.

### 5. Validation in a prospective clinical cohort

Risk stratification based on vascular habitat was applied to the prospective clinical cohort for validation. The Kaplan–Meier survival curve and risk table based on vascular habitat risk stratification is shown in Figure 5. Seven patients (46.7%, 7/15) were stratified to be poor responders while 8 patients (53.3%, 8/15) were stratified to be good responders. One patient (11.1%, 1/9) showed local enhancing pattern of progression and 6 patients (66.7%, 6/9) showed diffuse nonenhancing pattern of progression while 2 patients (22.2%, 2/9) showed distant progression. Patients exhibited a trend to be stratified as poor or good responders using vascular habitat score (log rank test,  $P = .059$ )

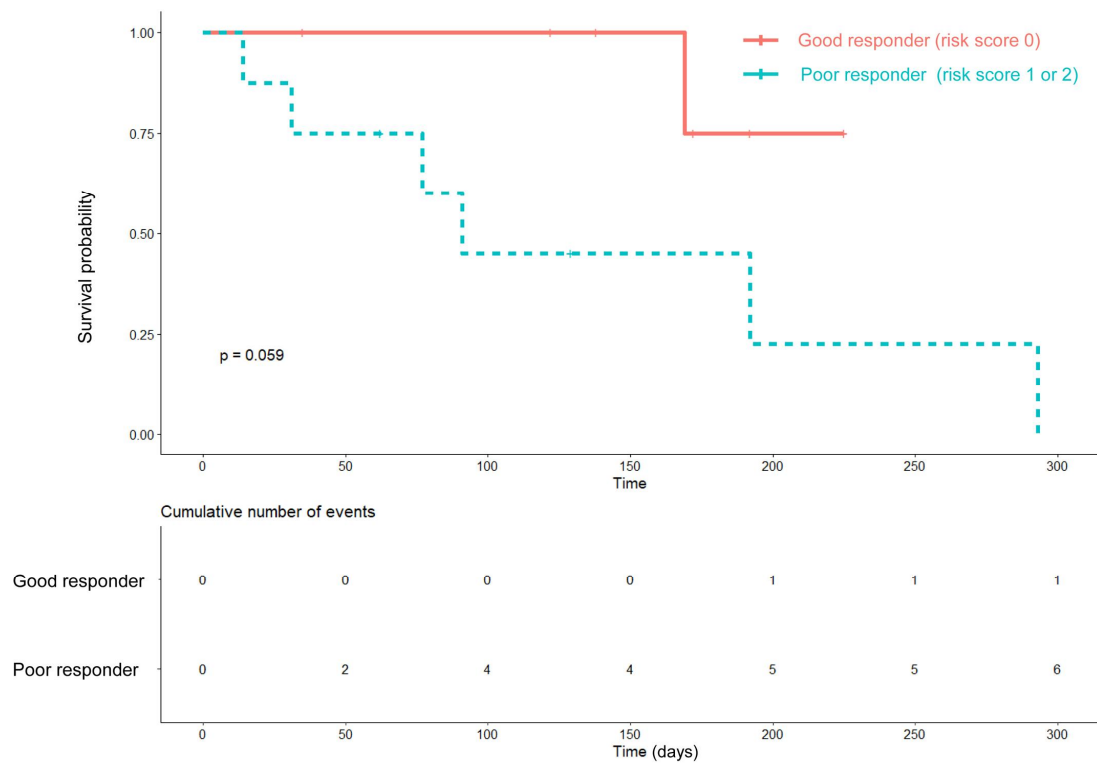


**Figure 5.** Risk stratification to good or poor responders based on high and intermediate angiogenic habitats showed a trend for predicting treatment resistance to bevacizumab therapy in the validation set.

## 고찰

In this study, we demonstrated that in recurrent glioblastomas treated with anti-angiogenic therapy, TTP could be predicted by perfusion- and vessel size-derived vascular habitat analysis. Not only high angiogenic habitat with high rCBV and vessel size but intermediate angiogenic habitat with intermediate rCBV and vessel size were significantly associated with treatment resistance and shorter TTP. The parcellation of vascular habitats enabled to more precisely predict treatment response than a well-known perfusion parameter of rCBV. This was validated in a prospective clinical cohort and vascular habitat analysis revealed a trend for predicting treatment resistance to anti-angiogenic therapy.



Previous studies examined perfusion parameters as a potential prognostic imaging biomarker of anti-angiogenic therapy in recurrent glioblastoma<sup>7-9</sup>. DSC-derived rCBV was most frequently explored, and pretreatment rCBV and histogram analysis of rCBV were shown to predict progression-free survival and overall survival<sup>7,8</sup>. In addition, voxel-based quantitative image features derived from rCBV were clustered to identify prognostic patient subgroups for survival and response to anti-angiogenic therapy<sup>9</sup>. Our study was an explorative analysis of perfusion- and vessel size-derived vascular habitat, and high angiogenic vascular habitat was most significantly associated with a shorter TTP (HR, 2.78; 95% CI, 1.53 – 5.02;  $P < .001$ ) with stronger association than rCBV (HR, 2.15; 95% CI, 1.10 – 4.17;  $P = .02$ ).

Vascular habitat incorporated information of perfusion parameter from DSC MRI and vessel size from VAI enabling more sophisticated illustration of complex tumor vascularity in recurrent glioblastoma<sup>21</sup>. By clustering voxels according to rCBV and vessel size into high, intermediate, and low angiogenic vascular habitats, vascular habitats better reflect the complex interplay of vascular mimicry, co-option and vasculogenesis in tumor vasculature<sup>11,22,23</sup>. In our study, both high and intermediate angiogenic habitats were significantly associated with shorter TTP, and risk stratification was based on high and intermediate angiogenic habitats. By applying cut-offs to high and intermediate angiogenic vascular habitats and excluding low angiogenic vascular habits, risk stratification was tailored to analyzing tumor microvasculature.

Our study showed that high and intermediate angiogenic vascular habitats characterized by large and intermediate vessel size were significant predictors of treatment resistance to anti-angiogenic therapy. Previous studies explored the significance of vessel size in recurrent glioblastoma<sup>10,15,24</sup>, and there was a higher proportion of larger vessels representing deoxygenated, venule-like vessels in recurrent glioblastoma<sup>10,24</sup>. The larger,

deoxygenated, venule-like vessels reflect nonuniform branching pattern of angiogenesis induced by tissue hypoxia with impaired vascular function<sup>25,26</sup>. This was targeted by anti-angiogenic therapy, and there was a reduction of larger vessels with slow inflow and an increase of vessels with fast inflow following anti-angiogenic therapy ultimately resulting in improved vascular function<sup>10,27</sup>. Higher proportion of vessels with large and intermediate size prior to initiation of anti-angiogenic therapy represents tissue hypoxia and impaired vascular function, and was able to predict treatment resistance to anti-angiogenic therapy. Previous studies included longitudinal analyses of VAI parameters in recurrent glioblastomas and bevacizumab-treated recurrent glioblastomas<sup>10,24</sup>, and consideration of follow-up time point in interpreting changes in VAI parameters is critical as vascular normalization is thought to peak at an expected time interval.

There were several limitations in this study. First, there was a small number of patients from a single center in the validation set. The vessel architecture imaging is not a widely available imaging protocol because of requirement of dual echo and machine compatibility. Therefore, further validation of cut-offs for risk stratification is required in a multi-center, large cohort study. Second, vascular habitats constructed based on rCBV and vessel size need to be pathologically confirmed for its spatial localization for future targeted therapy. However, while microvascular density and vessel size may be evaluated pathologically, spatial correlation would be technically challenging to achieve.

## 결론

In conclusion, perfusion- and vessel size-derived vascular habitat analysis predicted TTP in recurrent glioblastoma treated with anti-angiogenic therapy. High angiogenic and intermediate angiogenic habitats may better reflect the complex tumor vasculature of recurrent glioblastomas aiding patient stratification for anti-angiogenic therapy.

## 참고문헌

1. Sorensen AG, Emblem KE, Polaskova P, et al. Increased survival of glioblastoma patients who respond to antiangiogenic therapy with elevated blood perfusion. *Cancer research*. 2012; 72(2):402-407.
2. Batchelor TT, Gerstner ER, Emblem KE, et al. Improved tumor oxygenation and survival in glioblastoma patients who show increased blood perfusion after cediranib and chemoradiation. *Proceedings of the National Academy of Sciences of the United States of America*. 2013; 110(47):19059-19064.
3. Prados M, Cloughesy T, Samant M, et al. Response as a predictor of survival in patients with recurrent glioblastoma treated with bevacizumab. *Neuro-oncology*. 2011; 13(1):143-151.
4. Shapiro LQ, Beal K, Goenka A, et al. Patterns of failure after concurrent bevacizumab and hypofractionated stereotactic radiation therapy for recurrent high-grade glioma. *International journal of radiation oncology, biology, physics*. 2013; 85(3):636-642.
5. Nowosielski M, Wiestler B, Goebel G, et al. Progression types after antiangiogenic therapy are related to outcome in recurrent glioblastoma. *Neurology*. 2014; 82(19):1684-1692.
6. Cho SJ, Kim HS, Suh CH, Park JE. Radiological Recurrence Patterns after Bevacizumab Treatment of Recurrent High-Grade Glioma: A Systematic Review and Meta-Analysis. *Korean J Radiol*. 2020; 21(7):908-918.
7. Kickingereder P, Wiestler B, Burth S, et al. Relative cerebral blood volume is a potential predictive imaging biomarker of bevacizumab efficacy in recurrent glioblastoma. *Neuro-oncology*. 2015; 17(8):1139-1147.
8. Bennett IE, Field KM, Hovens CM, et al. Early perfusion MRI predicts survival outcome in patients with recurrent glioblastoma treated with bevacizumab and carboplatin. *Journal of neuro-oncology*. 2017;

- 131(2):321–329.
9. Liu TT, Achrol AS, Mitchell LA, et al. Magnetic resonance perfusion image features uncover an angiogenic subgroup of glioblastoma patients with poor survival and better response to antiangiogenic treatment. *Neuro-oncology*. 2017; 19(7):997–1007.
  10. Emblem KE, Mouridsen K, Bjornerud A, et al. Vessel architectural imaging identifies cancer patient responders to anti-angiogenic therapy. *Nature Medicine*. 2013; 19(9):1178–1183.
  11. Carmeliet P, Jain RK. Molecular mechanisms and clinical applications of angiogenesis. *Nature*. 2011; 473(7347):298–307.
  12. Stadlbauer A, Marhold F, Oberndorfer S, et al. Metabolic Tumor Microenvironment Characterization of Contrast Enhancing Brain Tumors Using Physiologic MRI. *Metabolites*. 2021; 11(10).
  13. O'Connor JP, Rose CJ, Waterton JC, Carano RA, Parker GJ, Jackson A. Imaging intratumor heterogeneity: role in therapy response, resistance, and clinical outcome. *Clinical cancer research : an official journal of the American Association for Cancer Research*. 2015; 21(2):249–257.
  14. Boxerman JL, Schmainda KM, Weisskoff RM. Relative cerebral blood volume maps corrected for contrast agent extravasation significantly correlate with glioma tumor grade, whereas uncorrected maps do not. *AJNR Am J Neuroradiol*. 2006; 27(4):859–867.
  15. Stadlbauer A, Eyüpoglu I, Buchfelder M, et al. Vascular architecture mapping for early detection of glioblastoma recurrence. *Neurosurgical focus*. 2019; 47(6):E14.
  16. Isensee F, Schell M, Pflueger I, et al. Automated brain extraction of multisequence MRI using artificial neural networks. *J Time Ser Anal*. 2019; 40(6):4952–4964.
  17. Gull SF. Bayesian Inductive Inference and Maximum Entropy. In: Erickson GJ, Smith CR, eds. *Maximum-Entropy and Bayesian Methods in Science and Engineering: Foundations*. Dordrecht: Springer

Netherlands; 1988:53–74.

18. Wen PY, Macdonald DR, Reardon DA, et al. Updated Response Assessment Criteria for High-Grade Gliomas: Response Assessment in Neuro-Oncology Working Group. *Journal of Clinical Oncology*. 2010; 28(11):1963–1972.
19. Pope WB, Xia Q, Paton VE, et al. Patterns of progression in patients with recurrent glioblastoma treated with bevacizumab. *Neurology*. 2011; 76(5):432–437.
20. Ingrisch M, Schneider MJ, Norenberg D, et al. Radiomic Analysis Reveals Prognostic Information in T1-Weighted Baseline Magnetic Resonance Imaging in Patients With Glioblastoma. *Invest Radiol*. 2017; 52(6):360–366.
21. Pries AR, Höpfner M, le Noble F, Dewhirst MW, Secomb TW. The shunt problem: control of functional shunting in normal and tumour vasculature. *Nat Rev Cancer*. 2010; 10(8):587–593.
22. Donnem T, Hu J, Ferguson M, et al. Vessel co-option in primary human tumors and metastases: an obstacle to effective anti-angiogenic treatment? *Cancer Med*. 2013; 2(4):427–436.
23. Seano G, Jain RK. Vessel co-option in glioblastoma: emerging insights and opportunities. *Angiogenesis*. 2020; 23(1):9–16.
24. Kim M, Park JE, Emblem K, Bjørnerud A, Kim HS. Vessel Type Determined by Vessel Architectural Imaging Improves Differentiation between Early Tumor Progression and Pseudoprogression in Glioblastoma. 2021.
25. Goel S, Duda DG, Xu L, et al. Normalization of the vasculature for treatment of cancer and other diseases. *Physiological reviews*. 2011; 91(3):1071–1121.
26. Wilson WR, Hay MP. Targeting hypoxia in cancer therapy. *Nature Reviews Cancer*. 2011; 11(6):393–410.
27. Sorensen AG, Batchelor TT, Zhang WT, et al. A "vascular normalization

index" as potential mechanistic biomarker to predict survival after a single dose of cediranib in recurrent glioblastoma patients. *Cancer research*. 2009; 69(13):5296-5300.

## 영문요약

**Vessel size and perfusion-derived vascular habitat refines prediction of resistance to bevacizumab in recurrent glioblastomas: validation in a prospective cohort**

**Author:** Minjae Kim, MD. Department of Radiology and the Research Institute of Radiology, University of Ulsan College of Medicine, Asan Medical Center.

**Background:** Anti-angiogenic therapy may not benefit all patients with recurrent glioblastomas, and imaging biomarker predicting treatment response to anti-angiogenic therapy is currently limited. We aimed to develop and validate vascular habitats based on perfusion and vessel size to predict time to progression (TTP) in patients with recurrent glioblastomas treated with bevacizumab.

**Methods:** Sixty-nine patients with recurrent glioblastomas treated with bevacizumab who underwent pretreatment MRI with dynamic susceptibility contrast imaging and vessel architectural imaging were enrolled. Vascular habitats were constructed using vessel size index (VSI) and relative cerebral blood volume (rCBV). Associations with vascular habitats and TTP were analyzed using Cox proportional hazard regression analysis. In a prospectively enrolled validation cohort consisting of 15 patients (ClinicalTrials.gov identifier; NCT04143425), stratification of TTP was demonstrated by Kaplan-Meier method (log-rank test) using vascular habitats.

**Results:** Three vascular habitats consisting of high, intermediate and low angiogenic habitats were identified with rCBV and VSI. Both high angiogenic and intermediate angiogenic habitats were significantly associated with a shorter TTP (hazard ratio [HR], 2.78 and 1.82, respectively; largest  $P = .003$ ). High angiogenic habitat demonstrated stronger predictive value than rCBV (HR, 2.15). Concordance probability index of vascular habitat combining high and intermediate angiogenic habitats was slightly higher than rCBV alone (0.74 vs.

0.72). Vascular habitats stratified patients to good or poor responder in a prospective cohort ( $P = .059$ ).

**Conclusions:** Perfusion- and vessel size-derived vascular habitats predicted TTP in recurrent glioblastomas treated with anti-angiogenic therapy and aided patient stratification in a prospective validation cohort.